Wearable System-on-a-Chip Pulse Radar Sensors for the Health Care: System Overview

Domenico Zito, Domenico Pepe, Bruno Neri,
Radio-frequency and Microwave Integrated Circuits Laboratory (RFLab),
Dept. of Information Engineering (DIIEIT),
University of Pisa,
56122 Pisa, Italy
Email: d.zito@iet.unipi.it

Danilo De Rossi, Antonio Lanatà,
Interdepartmental Research, Center E. Piaggio,
University of Pisa,
56122 Pisa, Italy

***Abstract*— A new system-on-a-chip radar sensor for next generation wearable wireless interface applied to the human health-care and safeguard is presented. The system overview is provided and a summary of the feasibility study of the radar sensor is presented. In detail, the overall system consists of a radar sensor for detecting the heart and breath rates and a low-power IEEE 802.15.4 ZigBee radio interface, which provides a wireless data link with remote data acquisition and control units. Particularly, the pulse radar exploits 3.1-10.6 GHz ultra wide band signals, which allow a significant reduction of the transceiver complexity and, then, of its power consuption. The operating principle is highlighted and the results of the system analysis are summarized. Such a novel system-on-a-chip wireless wearable interface enables low-cost silicon technologies for contactless measuring of the primary vital signs and extends the capability in terms of applications for the emerging wireless body area networks.**

I. Introduction

The recent advances in the standard CMOS silicon technologies has led up to highly miniaturized, low cost, and ultra low power integrated circuits. This fact allows the realization of high-potential systems-on-a-chip for a large number of new applications. One of the most interesting fields of application of fully integrated systems-on-chip is represented by the emerging wireless body area networks (WBANs) for the human health care and safeguard.

The paper focuses this topic and reports the idea of a novel wearable wireless interface for monitoring of the heart wall, for a contactless detection of the heart and breath rates.

The paper is organized as follows. In Section II, the idea of the next generation wearable interface for the human health-care and safeguard is presented. In Section III, the feasibility study of an ultra-wide-band (UWB) radar sensor for monitoring the heart and breath rates is summarized. Finally, in Section IV, the conclusions are drawn.

II. Wereable Wireless Interface for Heart Monitoring: System Overview

In February 2002 the Federal Communications Commission (FCC) gave the permission for the marketing and operation of a new class of products incorporating ultra-wide-band (UWB) technology [1]. The FCC, through a modification of the 47 CRF Part 15 regulations [2], decided the allocation of the UWB systems in a unlicensed band 7.5 GHz wide, in the range of the radiofrequency spectrum 3.1-10.6 GHz. Since UWB systems are intended to operate in regions of spectrum in which other services are already operating, the mask of the maximum power spectral density (PSD) allowed for UWB devices has been set to very low values (-41.3 dBm/MHz in the 3.1-10-6 GHz band).

One of the most promising class of applications of the UWB systems consists of the medical imaging. Particularly, a UWB radar sensor can be employed to monitor the heart wall and chest movements, in order to detect in real time the heart and breath rates, respectively.

The modern silicon technologies (the transistors of the standard CMOS 90 nm technology have cut-off frequencies higher than 150 GHz) allow us to realize ultra-small and ultra-low-power wireless UWB sensors for WBAN applications. WBANs consist of sensor networks, in which the sensors are placed around the human body in order to monitor constantly the vital parameters. The information collected by these sensors can be sent, by means of radio-frequency data link, toward a remote data acquisition and signal processing units or even to a personal server, which can forward the data to the medical centers and hospitals by means of internet. In this way, the medical staff can investigate on the manifesting of the heart deseases over the all daily activity of the subject under observation.

The overall system idea is shown Fig. 1. It consists of a fully integrated UWB radar sensor and a low-power radio interface. Both for the radar system and radar interface, we deal with their realization by means of a standard CMOS 90 nm by STMicroelectronics (STM).

In the scheme of Fig. 1 each antenna is realized on a microstrip substrate; however, in a most advanced realization, they can be realized directly by means of proper conductive layers tissued within clothes [3]. The data acquired by the radar sensor are transferred to a personal or remote unit by means of the low-power radio data link realized by a wireless transceiver based on the IEEE 802.15.4 (ZigBee) standard. This increases the flexibility of the wireless sensors, which

21st International Conference on Advanced Information Networking and Applications Workshops (AINAW'07)
0-7695-2847-3/07 $20.00 © 2007 IEEE

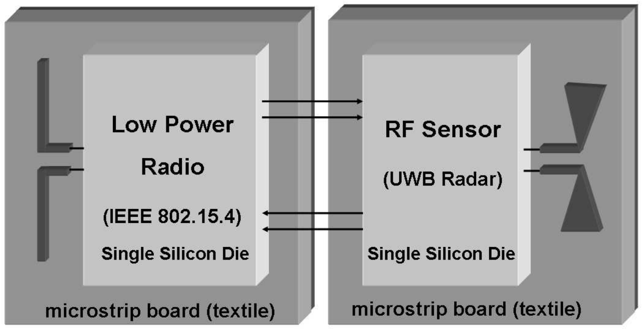

Fig. 1. Wereable wireless interface for the heart monitoring: system idea.

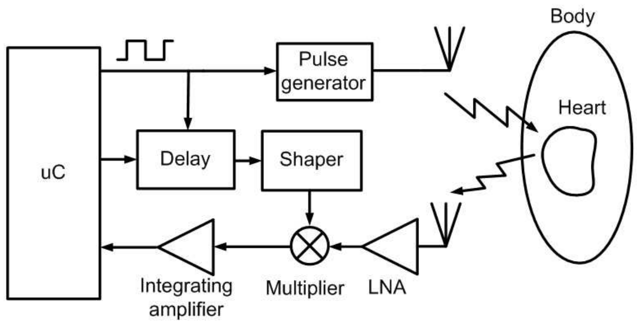

Fig. 2. Block diagram of the proposed fully integrated UWB radar for the detection of heart and breath rates.

can be reconfigured in real time by acting on the control unit of the wireless network.

The proposed fully integrated UWB radar (Fig. 2) detects the heart and breath rates by sending very short electromagnetic pulses (hundreds of picoseconds) and detecting the echoes generated by the reflections at the heart wall (due to the different characteristic impedances between the heart muscle and the blood flowing inside the heart itself). A basic principle of operation is described in [4], [5].

It is worth mentioning that, the UWB pulses (3.1-10.6 GHz) are not influenced by clothes or blankets and they can be exploited efficiently for the monitoring of the heart rate [5].

Moreover, the UWB pulses have a very low-density spectrum that, if compared with the narrow band conterparts, reduce drastically the risk of cellular ionization on the animal and human beings [6]–[11]. In addition, since UWB transceivers present a lower circuit complexity, the requirements in term of power consumption are mitigated, and this allows us to maximize the energy saving for a longer life of the battery.

III. System-on-a-chip UWB Radar Sensor for the Heart and Breath Rates Monitoring

The main block of the proposed wereable wireless interface for the monitoring of the heart is represented by the UWB radar sensor. The radar architecture is shown in Fig. 2.

A correlator-type topology has been adopted for the receiver. The cross-correlator has a frequency response equal to that of a matched filter. It can be demonstrated that the matched filter is the proper filter which provides the best signal-to-noise ratio (SNR, it is the ratio between the signal power and the noise power) at the output. Moreover, preliminary results obtained with the Ptolemy simulator, within the CAD tool ADS2005A™ by Agilent Technologies, have shown that the correlator-type receiver allows the achievement of the best SNR at the output of the receiver front-end (Low Noise Amplifier (LNA) and multiplier) with respect to other topologies and, moreover, the highest sensitivity for small excursions of the heart wall.

In detail, the system operates by sending extremely short electromagnetic pulses toward the heart. Due to the different characteristic impedance of the two media, a part of the incident energy is reflected at the interface between the heart muscle and the blood which flows inside, due to the different characteristic impedances of the two media. After a delay equal to the time-of-flight of the pulse, from the radar to the heart and then again to the radar, a delayed replica of the transmitted pulse is correlated with the echo received from the heart wall. The delay can be digitally programmable (to be remotely set as well), in order to calibrate properly the wearable device on the person under observation and extend its adaptibility over the all range of the anatomical variability of the population.

A pulse repetition frequency (PRF) greater than 1 MHz allows us to consider the heart almost motionless between two consecutive pulses.

The voltage amplitude of the output signal of the multiplier reaches the maximum when the received echo and the delayed local replica of the transmitted pulse are perfectly time-aligned. Then, the amplitude of the signal at the output of the multiplier is related to the heart position.

The output voltage of the receiver front-end is averaged by integrating over a large number of pulses. This operation allows us to increase significantly the signal-to-noise ratio at the output of the receiver. Moreover, the amplitude of the continuous output signal of the integrator is related to the time-varying position of the moving object under observation (the heart wall, in our case). Thus, the output signal provided by the integrator includes the tones of the heart beat and the breathing frequency.

A. *Summary of the Feasibility Study of the UWB Radar Sensor*

In order to demonstrate the feasibility of such a UWB radar sensor, a system analysis has been carried out by means of both theoretical model and CADtool simulations.

Firstly, we developed a theoretical model of the channel in which the pulse propagates. The properties of the body tissues have been extracted by the parametric models developed by C. Gabriel and his collegues at the Brooks Air Force Base (U.S.A.) [12], [13]. As for the layers, we considered the model proposed in [5], which is based on the Visible Human Project and the Gabriel's data book. The loss channel model has been derived taking into account i) path loss, ii) attenuation in the tissues and iii) losses due to the reflections at the

0-7695-2847-3/07 $20.00 © 2007 IEEE

interface between different tissues. Near field equations have been employed to carry out the analysis, since the UWB radar sensor operates in proximity of the human chest. The overall losses result equal to about 60 dB at 3 GHz and they became higher as the frequency rises (about 160 dB at 10 GHz). Simulation results have shown that the average power loss of the pulse in the 3.1-10.6 GHz band is aproximately equal to 80 dB.

Then, the specifications of the building blocks have been derived taking into account the characteristic performance of the standard process CMOS 90 nm by STM, which has been considered for their implementation on silicon.

As for the transmitter, the pulse transmitted has to be very short in order to obtain resolution range in the order of a few centimeters as such as the maximum displacement of the heart wall. A PRF between 1 and 10 MHz allow us to reach the compliance with the FCC mask for the maximum level of emitted power.

Then the specifications for the radar receiver have been derived. The minimum power (S_{min}) of a received signal which allows the achievement of a given SNR (SNR_{out}) at the output of the receiver can be estimated as follows:

$$S_{min} = k \times T \times B \times NF \times SNR_{out} \quad (1)$$

where k is the Boltzmann's constant (1.38×10^{-23} J/K), T is the antenna noise temperature, NF is the receiver noise figure and B is the receiver bandwidth. Considering that the average channel loss in the 3.1-10.6 GHz band is equal to 80 dB, a noise figure lower than -11.5 dB would be required in order to have an output SNR (for a single pulse) of at least 10 dB.

The output SNR of a radar receiver is increased by integrating several pulses received. Since the frequencies of the vital parameters of interest are in the order of Hz, an integrator with a band of 100 Hz allows us to properly capture these tones. However, in order to reduce the overall simulation time, a band of 1 KHz has been considered in the following. For a PRF equal to 10 MHz, 10000 pulses at a time are averaged. From the tables available in [14], it can be seen that an integration over 10000 pulses allows an improvement of the SNR at the output of the receiver of about 40 dB. This result is confirmed by the rough estimation provided by the equation (2)

$$SNR_{imp} = 10 \times \log\left(\frac{B}{PRF}\right) = +40 \text{ dB} \quad (2)$$

Thus, the integrations of a large number of pulses relaxes the receiver front-end (low noise amplifier and multiplier) specifications. The noise figure of the overall receiver front-end has to be lower than

$$NF_{max} = -11.5 + 40 = 28.5 \text{ dB} \quad (3)$$

Thus, the specifications for the LNA (low noise amplifier), the multiplier and the integrator blocks have been derived.

In order to validate the theoretical model of the radar, the overall system has been simulated with the Ptolemy simulator within Agilent ADS2005A™. Each building block

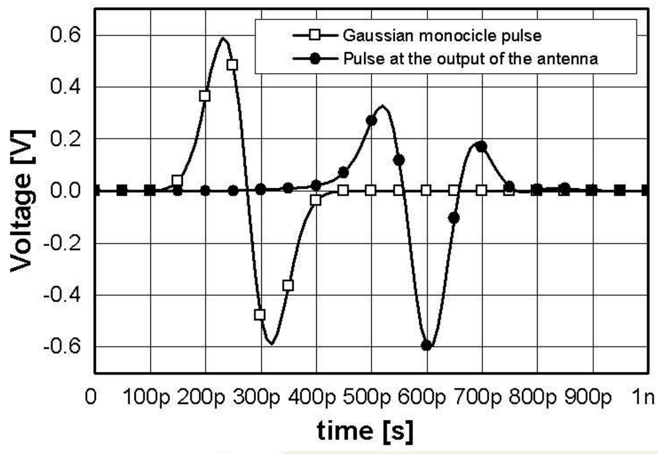

Fig. 3. The gaussian monocycle pulse of 1.2 Volts peak-to-peak generated by the transmitter and the signal at the output of the antenna filter.

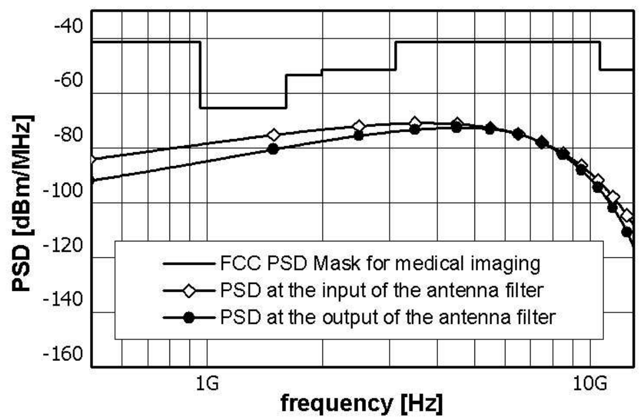

Fig. 4. Power Spectral Density (PSD) of the train of gaussian monocycle pulses (200 ps short and 1.2 Volts peak-to-peak wide each) with a PRF of 1 MHz and that obtained at the output the antenna filter.

was characterized by frequency response and noise contribution achievable realistically with the CMOS 90 nm process. Simulation results have confirmed the feasibility of a fully integrated system-on-a-chip UWB radar sensor on silicon. The most representative results are reported in Figg. 3, 4, 5, 6. The gaussian monocycle pulse generated by the transmitter and the pulse at the output of the antenna filter are shown in Fig. 3. The power spectral density (PSD) of a train of a sequence (train) of pulses (200 ps short and 1.2 Volts peak-to-peak wide each) with a PRF equal to 1 MHz is shown reported in Fig. 4, both for the input and output of the antenna filter. Note that the radar signal is compliant with the FCC mask for the UWB medical imaging systems.

The voltage (noise inclusive) at the input of the LNA is shown in Fig. 5.

The voltage at the output of the integrator is shown in Fig. 6. This signal has the same frequency of the time-varying surface (i.e. the heart wall) under observation. A heart movement having a period of 20 ms has been considered. This period

21st International Conference on
Advanced Information Networking and Applications Workshops (AINAW'07)
0-7695-2847-3/07 $20.00 © 2007 IEEE

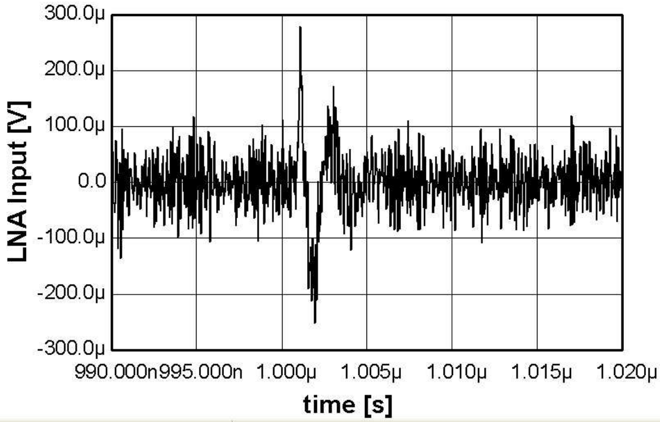

Fig. 5. Voltage signal at the input of the LNA (noise inclusive).

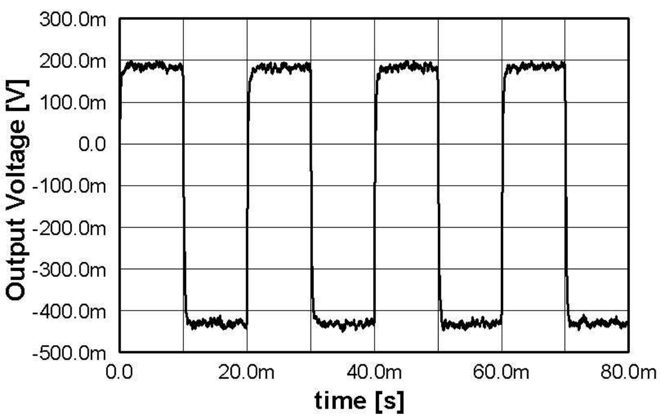

Fig. 6. Output voltage of the integrator filter of the radar sensor. The output signal has the same frequency of the movement imposed for the heart wall. A time-varying surface with a period of 20 ms has been considered for the simulation (this period is short with respect to the real heart moving, in order to reduce the simulation time. This does not impair the analysis since the radar reaches widely the steady state within ten ms).

has been compressed with respect to the real heart movement in order to reduce the simulation time. This does not impair the analysis since the radar reaches widely the steady state within ten milliseconds. Simulation results show that the increase of the SNR from the output of the multiplier to the output of the integrator is of about 40 dB, as predicted in the theoretical system analyses.

IV. Conclusion

The recent advances in silicon CMOS technology allow the realization of more and more miniaturized, low-cost and low-power integrated system-on-a-chip sensors. These sensors can be employed in the wireless body area networks, for advanced and continuos monitoring of vital parameters.

Particularly, the system overview of a next generation wearable wireless sensors for human health care and safeguard has been presented herein. Such a system is composed by a novel fully integrated ultra-wide-band radar sensor for the detection of the heart and breath rates and a low-power radio interface (IEEE 802.15.4, ZigBee), which collects the data provided by the sensor and sends these data to an aquisition unit or even in internet by means of a personal server. Thus, the physiological data of a person inder observation (e.g. a patient) can be sent in real time to the hospital and, then, the doctors could act in-time in case of anomalies in the vital parameters monitored.

A detailed feasibility study of the UWB radar on silicon technology (CMOS 90 nm) has been carried out, by means of both theoretical and CAD tool simulations. The simulation results have shown a wide agreement with the theoretical model of the radar, demonstrating the feasibility of the proposed single-chip radar sensor on a modern silicon technology.

Present and future works are addressed to the antenna design, channel model verification by means of measurements, building blocks design and their co-integration, system-on-a-chip prototyping and experimental characterization.

Acknowledgment

The authors are grateful to the European Community for its financial support through the EU project ProeTEX within the 6th Framework Programme.

References

[1] "New public safety applications and broadband internet access among uses envisioned by fcc authorization of ultra-wideband technology," Federal Communications Commission, 2002. [Online]. Available: http://www.fcc.gov/Bureaus/Engineering_Technology/News_Releases/2002/nret0203.html
[2] "47 cfr part 15," Federal Communications Commission, 2002. [Online]. Available: http://www.fcc.gov/oet/info/rules/
[3] M. Klemm and G. Troester, "Textile uwb antennas for wireless body area networks," *IEEE Transaction on Antennas and Propagation*, vol. 54, no. 11, pp. 3192–3197, Nov. 2006.
[4] T. E. McEwan, "Body monitoring and imaging apparatus and method," U.S. Patent 5 573 012, Nov. 12, 1996.
[5] E. M. Staderini, "Uwb radars in medicine," *IEEE Aerospace and Electronic Systems Magazine*, vol. 17, no. 1, pp. 13–18, Jan. 2002.
[6] S. F. Cleary, F. Nickless, L. M. Liu, and R. Hoffman, "Studies of exposure of rabbits to electromagnetic pulsed fields," *Bioelectromagnetics*, vol. 1, no. 3, pp. 345–352, 1980.
[7] J. A. D'Andrea, B. L. Cobb, and J. O.Lorge, "Lack of behavioral effects in the rhesus monkey: high peak microwave pulses at 1.3 ghz," *Bioelectromagnetics*, vol. 10, no. 1, pp. 65–76, 1989.
[8] T. J. Walters, P. Mason, C. Sherry, C. Steffen, and J. H. Merritt, "No detectable bioeffects following acute exposure to high peak power ultra-wide band electromagnetic radiation in rats," *Aviat. Space Environ. Med.*, vol. 66, no. 6, pp. 562–567, June 1995.
[9] C. J. Sherry, D. W. Blick, T. J. Walters, and G. C. Brown, "Lack of behavioral effects in non-human primates after exposure to ultrawideband electromagnetic radiation in the microwave frequency range," *Radiat. Res.*, vol. 143, no. 1, pp. 93–97, July 1995.
[10] J. Merritt, J. L. Gel, and W. D. Hurt, "Considerations for human exposure standards for fast-rise-time high-penk-power electromagnetic pulses," *Aviat. Space Environ. Med.*, vol. 6, no. 66, pp. 586–589, June 1995.
[11] J. R. Jauchem, R. L. Seaman, H. M. Lehnert, S. P. Mathur, K. L. Ryan, M. R. Frei, and W. D. Hurt, "Ultra-wideband electromagnetic pulses: lack of effects on heart rate and blood pressure during two-minute exposures of rats," *Bioelectromagnetics*, vol. 19, no. 5, pp. 330–333, 1998.
[12] C. Gabriel and S. Gabriel, "Compilation of the dielectric properties of body tissues at rf and microwave frequencies," 2002. [Online]. Available: http://www.brooks.af.mil/AFRL/HED/hedr/reports/dielectric/home.html
[13] D. Andreuccetti, R. Fossi, and C. Petrucci, "Calculation of the dielectric properties of body tissues in the frequency range 10 hz - 100 ghz," 2002. [Online]. Available: http://niremf.ifac.cnr.it/tissprop/htmlclie/stfrtag
[14] M. I. Skolnik, *Radar Handbook*. McGraw Hill Book Company, 1970.

IEEE COMPUTER SOCIETY

View publication stats